

# World Journal of *Gastroenterology*

*World J Gastroenterol* 2021 March 28; 27(12): 1117-1254



**REVIEW**

- 1117 Cascade of care for children and adolescents with chronic hepatitis C  
*Rogers ME, Balistreri WF*

**MINIREVIEWS**

- 1132 Primary localized gastric amyloidosis: A scoping review of the literature from clinical presentations to prognosis  
*Lin XY, Pan D, Sang LX, Chang B*
- 1149 Emerging wearable technology applications in gastroenterology: A review of the literature  
*Chong KP, Woo BK*

**ORIGINAL ARTICLE****Retrospective Cohort Study**

- 1161 Perioperative blood transfusion decreases long-term survival in pediatric living donor liver transplantation  
*Gordon K, Figueira ERR, Rocha-Filho JA, Mondadori LA, Joaquim EHG, Seda-Neto J, da Fonseca EA, Pugliese RPS, Vintimilla AM, Auler Jr JOC, Carmona MJC, D'Albuquerque LAC*

**Retrospective Study**

- 1182 R2\* value derived from multi-echo Dixon technique can aid discrimination between benign and malignant focal liver lesions  
*Shi GZ, Chen H, Zeng WK, Gao M, Wang MZ, Zhang HT, Shen J*
- 1194 Cytapheresis re-induces high-rate steroid-free remission in patients with steroid-dependent and steroid-refractory ulcerative colitis  
*Iizuka M, Etou T, Shimodaira Y, Hatakeyama T, Sagara S*

**Observational Study**

- 1213 Risk perception and knowledge of COVID-19 in patients with celiac disease  
*Zhen J, Stefanolo JP, Temprano MDLP, Seiler CL, Caminero A, de-Madaria E, Huguet MM, Santiago V, Niveloni SI, Smecuol EG, Domínguez LU, Trucco E, Lopez V, Olano C, Mansueto P, Carroccio A, Green PH, Duerksen D, Day AS, Tye-Din JA, Bai JC, Ciacci C, Verdú EF, Lebowl B, Pinto-Sanchez MI*
- 1226 Risk stratification and geographical mapping of Brazilian inflammatory bowel disease patients during the COVID-19 outbreak: Results from a nationwide survey  
*Queiroz NSF, Teixeira FV, Motta MP, Chebli LA, Hino AAF, Martins CA, Quaresma AB, Silva AAPD, Damião AOMC, Saad-Hossne R, Kotze PG*

**META-ANALYSIS**

**1240** Hepatitis E in solid organ transplant recipients: A systematic review and meta-analysis

*Hansrivijit P, Trongtorsak A, Puthenpura MM, Boonpheng B, Thongprayoon C, Wijarnpreecha K, Choudhury A, Kaewput W, Mao SA, Mao MA, Jadlovec CC, Cheungpasitporn W*

**ABOUT COVER**

Editorial Board Member of *World Journal of Gastroenterology*, Kai Wang, MD, PhD, Professor, Discipline Leader of Department of Hepatology, Qilu Hospital of Shandong University, Director of Hepatology Institute of Shandong University, No. 107 Wenhua Road, Jinan 250012, Shandong Province, China. wangdoc2010@163.com

**AIMS AND SCOPE**

The primary aim of *World Journal of Gastroenterology* (*WJG*, *World J Gastroenterol*) is to provide scholars and readers from various fields of gastroenterology and hepatology with a platform to publish high-quality basic and clinical research articles and communicate their research findings online. *WJG* mainly publishes articles reporting research results and findings obtained in the field of gastroenterology and hepatology and covering a wide range of topics including gastroenterology, hepatology, gastrointestinal endoscopy, gastrointestinal surgery, gastrointestinal oncology, and pediatric gastroenterology.

**INDEXING/ABSTRACTING**

The *WJG* is now indexed in Current Contents®/Clinical Medicine, Science Citation Index Expanded (also known as SciSearch®), Journal Citation Reports®, Index Medicus, MEDLINE, PubMed, PubMed Central, and Scopus. The 2020 edition of Journal Citation Report® cites the 2019 impact factor (IF) for *WJG* as 3.665; IF without journal self cites: 3.534; 5-year IF: 4.048; Ranking: 35 among 88 journals in gastroenterology and hepatology; and Quartile category: Q2. The *WJG*'s CiteScore for 2019 is 7.1 and Scopus CiteScore rank 2019: Gastroenterology is 17/137.

**RESPONSIBLE EDITORS FOR THIS ISSUE**

Production Editor: Ji-Hong Lin, Production Department Director: Yun-Xiao Jian Wu, Editorial Office Director: Ze-Mao Gong.

**NAME OF JOURNAL**

*World Journal of Gastroenterology*

**ISSN**

ISSN 1007-9327 (print) ISSN 2219-2840 (online)

**LAUNCH DATE**

October 1, 1995

**FREQUENCY**

Weekly

**EDITORS-IN-CHIEF**

Andrzej S Tarnawski, Subrata Ghosh

**EDITORIAL BOARD MEMBERS**

<http://www.wjgnet.com/1007-9327/editorialboard.htm>

**PUBLICATION DATE**

March 28, 2021

**COPYRIGHT**

© 2021 Baishideng Publishing Group Inc

**INSTRUCTIONS TO AUTHORS**

<https://www.wjgnet.com/bpg/gerinfo/204>

**GUIDELINES FOR ETHICS DOCUMENTS**

<https://www.wjgnet.com/bpg/GerInfo/287>

**GUIDELINES FOR NON-NATIVE SPEAKERS OF ENGLISH**

<https://www.wjgnet.com/bpg/gerinfo/240>

**PUBLICATION ETHICS**

<https://www.wjgnet.com/bpg/GerInfo/288>

**PUBLICATION MISCONDUCT**

<https://www.wjgnet.com/bpg/gerinfo/208>

**ARTICLE PROCESSING CHARGE**

<https://www.wjgnet.com/bpg/gerinfo/242>

**STEPS FOR SUBMITTING MANUSCRIPTS**

<https://www.wjgnet.com/bpg/GerInfo/239>

**ONLINE SUBMISSION**

<https://www.f6publishing.com>

## Retrospective Study

**R2\* value derived from multi-echo Dixon technique can aid discrimination between benign and malignant focal liver lesions**

Guang-Zi Shi, Hong Chen, Wei-Ke Zeng, Ming Gao, Meng-Zhu Wang, Hui-Ting Zhang, Jun Shen

**ORCID number:** Guang-Zi Shi 0000-0003-0170-7895; Hong Chen 0000-0001-9057-3766; Wei-Ke Zeng 0000-0002-9869-7023; Ming Gao 0000-0003-4602-4393; Meng-Zhu Wang 0000-0001-5674-4162; Hui-Ting Zhang 0000-0002-2417-6874; Jun Shen 0000-0001-7746-5285.

**Author contributions:** Shi GZ and Chen H contributed equally to this work; Shi GZ and Shen J designed the research; Shi GZ, Chen H, Zeng WK, and Wang MZ collected and analyzed the data; Shi GZ wrote the manuscript; Shi GZ, Chen H, Zeng WK, Gao M, Wang MZ, and Zhang HT analyzed and interpreted the data; Shen J wrote and revised the manuscript; all co-authors participated in writing and checking the manuscript, and approved the submitted manuscript.

**Institutional review board**

**statement:** This study was reviewed and approved by the Ethics Committee of Sun Yat-Sen Memorial Hospital.

**Informed consent statement:**

Patients were not required to give informed consent to the study because the analysis used anonymous clinical data that were obtained after each patient agreed to treatment by written consent.

**Guang-Zi Shi, Hong Chen, Wei-Ke Zeng, Ming Gao, Jun Shen,** Department of Radiology, Sun Yat-Sen Memorial Hospital, Sun Yat-Sen University, Guangzhou 510120, Guangdong Province, China

**Meng-Zhu Wang, Hui-Ting Zhang,** MR Scientific Marketing, Siemens Healthineers, Guangzhou 510120, Guangdong Province, China

**Corresponding author:** Jun Shen, MD, Doctor, Professor, Department of Radiology, Sun Yat-Sen Memorial Hospital, Sun Yat-Sen University, No. 107 Yanjiang Road West, Guangzhou 510120, Guangdong Province, China. [shenjun@mail.sysu.edu.cn](mailto:shenjun@mail.sysu.edu.cn)

**Abstract****BACKGROUND**

R2\* estimation reflects the paramagnetism of the tumor tissue, which may be used to differentiate between benign and malignant liver lesions when contrast agents are contraindicated.

**AIM**

To investigate whether R2\* derived from multi-echo Dixon imaging can aid differentiating benign from malignant focal liver lesions (FLLs) and the impact of 2D region of interest (2D-ROI) and volume of interest (VOI) on the outcomes.

**METHODS**

We retrospectively enrolled 73 patients with 108 benign or malignant FLLs. All patients underwent conventional abdominal magnetic resonance imaging and multi-echo Dixon imaging. Two radiologists independently measured the mean R2\* values of lesions using 2D-ROI and VOI approaches. The Bland-Altman plot was used to determine the interobserver agreement between R2\* measurements. Intraclass correlation coefficient (ICC) was used to determine the reliability between the two readers. Mean R2\* values were compared between benign and malignant FLLs using the nonparametric Mann-Whitney test. Receiver operating characteristic curve analysis was used to determine the diagnostic performance of R2\* in differentiation between benign and malignant FLLs. We compared the diagnostic performance of R2\* measured by 2D-ROI and VOI approaches.

**RESULTS**

This study included 30 benign and 78 malignant FLLs. The interobserver reproducibility of R2\* measurements was excellent for the 2D-ROI (ICC = 0.994)

**Conflict-of-interest statement:** The authors declare no conflict of interest.

**Data sharing statement:** No additional data are available.

**Open-Access:** This article is an open-access article that was selected by an in-house editor and fully peer-reviewed by external reviewers. It is distributed in accordance with the Creative Commons Attribution NonCommercial (CC BY-NC 4.0) license, which permits others to distribute, remix, adapt, build upon this work non-commercially, and license their derivative works on different terms, provided the original work is properly cited and the use is non-commercial. See: <http://creativecommons.org/licenses/by-nc/4.0/>

**Manuscript source:** Unsolicited manuscript

**Specialty type:** Gastroenterology and hepatology

**Country/Territory of origin:** China

**Peer-review report's scientific quality classification**

Grade A (Excellent): 0  
Grade B (Very good): B, B  
Grade C (Good): 0  
Grade D (Fair): 0  
Grade E (Poor): 0

**Received:** November 20, 2020

**Peer-review started:** November 20, 2020

**First decision:** January 23, 2021

**Revised:** February 2, 2021

**Accepted:** February 25, 2021

**Article in press:** February 25, 2021

**Published online:** March 28, 2021

**P-Reviewer:** Pop TL

**S-Editor:** Zhang H

**L-Editor:** Wang TQ

**P-Editor:** Liu JH



and VOI (ICC = 0.998) methods. Bland–Altman analysis also demonstrated excellent agreement. Mean R2\* was significantly higher for malignant than benign FFLs as measured by 2D-ROI ( $P < 0.001$ ) and VOI ( $P < 0.001$ ). The area under the curve (AUC) of R2\* measured by 2D-ROI was 0.884 at a cut-off of 25.2/s, with a sensitivity of 84.6% and specificity of 80.0% for differentiating benign from malignant FFLs. R2\* measured by VOI yielded an AUC of 0.875 at a cut-off of 26.7/s in distinguishing benign from malignant FFLs, with a sensitivity of 85.9% and specificity of 76.7%. The AUCs of R2\* were not significantly different between the 2D-ROI and VOI methods.

## CONCLUSION

R2\* derived from multi-echo Dixon imaging whether by 2D-ROI or VOI can aid in differentiation between benign and malignant FLLs.

**Key Words:** R2\*; Multi-echo Dixon imaging; Hypoxia; Malignant lesion; Benign lesion; Focal liver lesion

©The Author(s) 2021. Published by Baishideng Publishing Group Inc. All rights reserved.

**Core Tip:** Our study showed that mean R2\* value of malignant focal liver lesions (FLLs) was significantly higher than that of benign FLLs. R2\* derived from multi-echo Dixon imaging is a potential biomarker to differentiate malignant from benign FFLs. The multi-echo Dixon sequence is easy to perform and requires only a single breath-hold of 16 s to image the entire liver, which holds a good potential for clinical application.

**Citation:** Shi GZ, Chen H, Zeng WK, Gao M, Wang MZ, Zhang HT, Shen J. R2\* value derived from multi-echo Dixon technique can aid discrimination between benign and malignant focal liver lesions. *World J Gastroenterol* 2021; 27(12): 1182-1193

**URL:** <https://www.wjgnet.com/1007-9327/full/v27/i12/1182.htm>

**DOI:** <https://dx.doi.org/10.3748/wjg.v27.i12.1182>

## INTRODUCTION

Liver cancer is the sixth most common cancer and the fourth leading cause of cancer deaths worldwide<sup>[1]</sup>. The liver is also the most frequent site for distant metastases<sup>[2]</sup>. Clinically, once a focal liver lesion (FLL) is identified, it is essential to distinguish between benign and malignant lesions, as this differentiation determines the individual's prognosis and subsequent treatment strategy<sup>[3]</sup>. Contrast-enhanced computed tomography (CT) and magnetic resonance imaging (MRI) are widely used to detect and characterize FLLs<sup>[4-7]</sup>. However, the use of iodine and gadolinium-based contrast agents is sometimes contraindicated; for example, in patients with severe kidney impairment due to the potential development of contrast-induced nephropathy<sup>[8]</sup> or nephrogenic systemic fibrosis<sup>[9]</sup>. Several imaging techniques without the need of contrast agents have been used to diagnose FFLs, including diffusion-weighted image (DWI), intravoxel incoherent motion, diffusion kurtosis imaging, and magnetic resonance elastography, although these techniques have shown mixed success with limited clinical application<sup>[10-13]</sup>.

A hypoxic microenvironment is a hallmark in biology for solid tumors<sup>[14,15]</sup>. It is known that R2\* estimation ( $R2^* = 1/T2^*$ ) is inversely related to partial tissue pressure of oxygen, and reflects the paramagnetism of the tumor tissue, such as the presence of deoxygenated hemoglobin<sup>[15-17]</sup>. Previous studies have demonstrated that R2\* can be used to assess oxygenation status in several malignancies<sup>[18,19]</sup> and offer additive value in identifying metastatic lymph nodes in breast cancer<sup>[20]</sup>. However, whether R2\* can be used to differentiate between benign and malignant FLLs remains to be determined. Besides, 2D region of interest (2D-ROI) and volume of interest (VOI) analyses, which are better for R2\* measurement in FFLs, remain elusive.

In this study, the diagnostic performances of R2\* derived from multi-echo Dixon imaging in differentiating between benign and malignant FLLs based on 2D-ROI and

VOI analyses were investigated. The purpose of this study was to determine whether R2\* derived from multi-echo Dixon imaging can aid in differentiating benign from malignant FLLs, and the impact of 2D-ROI and VOI on the outcomes.

## MATERIALS AND METHODS

### Patients

This retrospective study was approved by the Institutional Ethics Review Board of our hospital (approval No. SYSEC-KY-KS-2020-147), and the requirement for informed consent from the patients was waived. From January 2019 to December 2019, consecutive patients with FLLs were identified from the hospital database. Patients were included if they had: (1) A solid malignant or benign FLL confirmed by histology, and follow-up contrast-enhanced CT/MRI examination for at least 6 mo, or positron emission tomography (PET)-CT; and (2) Multi-echo Dixon imaging. The exclusion criteria were as follows: (1) Diffuse liver inflammation ( $n = 5$ ); (2) Maximal lesion diameter  $< 10$  mm ( $n = 5$ ); (3) Lower signal-to-noise ratio on R2\* images; and (4) Obvious breathing artifacts on R2\* images ( $n = 5$ ).

### MRI acquisition

MRI was performed on a 3.0 T unit (MAGNETOM Skyra; Siemens Healthcare, Erlangen, Germany). The sequences consisted of conventional sequences and multi-echo Dixon imaging. Conventional MRI included axial BLADE T2-weighted imaging (T2WI) [repetition-time/echo-time (TR/TE) = 9672.9-12331.7/84 ms; flip angle = 130°; averages = 1; matrix = 320 × 320; field of view = 100 mm; slice thickness = 5 mm], axial and coronal T1-weighted imaging (T1WI) volume interpolated breath-hold examination (VIBE) (TR/TE = 3.97/1.29 ms; flip angle = 9°; averages = 1; matrix = 320 × 180; field of view = 75 mm; slice thickness = 3 mm), and axial DWI (TR/TE = 4900/66 ms; flip angle = 90°; averages = 12; matrix = 192 × 113; field of view = 78.125 mm; slice thickness = 5 mm; b values = 0 and 800 s/m<sup>2</sup>). The multi-echo Dixon imaging was performed with T2\* correction. The acquisition parameters were: TR = 9 ms; six-echo with TE = 1.05/2.46/3.69/4.92/6.15/7.38 ms; averages = 1; matrix = 160 × 136; field of view = 450 mm; slice thickness = 3.5 mm; number of slices = 64; a flip angle = 4° was used to minimize the effects of T1 weighting<sup>[21]</sup>. This sequence was acquired in a breath-hold of 16 s. After these sequences, multiphase contrast-enhanced imaging was performed after administration of gadolinium contrast medium (Magnevist; Bayer Schering Pharma, Berlin, Germany) using a fat-suppressed dynamic contrast enhancement sequence with the following acquisition parameters: TR/TE = 3.8/1.23 ms; averages = 1; slice thickness = 2.5; field of view = 80.56; matrix = 288 × 186; flip angle = 10°. Then, all patients underwent axial and coronal contrast-enhanced T1WI-VIBE (TR/TE = 3.97/1.26 ms; flip angle = 9°; averages = 1; slice thickness = 2.3 mm; matrix = 320 × 180; field of view = 75 mm).

### Image analysis

All the images were assessed by using the ImageJ software (<http://rsb.info.nih.gov/ij/>). A low flip angle multi-echo Dixon sequence was used to derive R2\* to minimize T1-related bias and improve the separation of water and fat. The improved fitting of the signals within fatty tissues allows more accurate R2\* mapping and T2\* correction of the water-fat separation<sup>[22]</sup>. Two experienced radiologists (Shi GZ and Gao M, with 6 and 12 years of experience in liver diagnostic imaging, respectively) who were blinded to the diagnosis of patients manually delineated the lesions on R2\* maps. For 2D-ROI, a single freehand ROI was drawn to cover the whole tumor area on the section showing the maximal tumor dimension. For VOI, the freehand ROI was placed slice by slice to cover the entire tumor volume. The mean R2\* values measured by 2D-ROI and VOI were used for analysis (Figure 1).

### Laboratory and anthropometric evaluations

Hepatitis B virus infection,  $\alpha$ -fetoprotein (AFP), carbohydrate antigen 19-9 (CA 19-9), and carcinoma embryonic antigen (CEA) were measured using standard reagents. Liver cirrhosis was determined by Masson trichrome staining. The normal ranges are: AFP  $\leq 25$  ng/mL, CA 19-9  $\leq 34$  U/mL, and CEA  $\leq 5$  ng/mL. Laboratory examination was performed before clinical treatment. The time between laboratory examination and multi-echo MRI examination was within 1 wk.

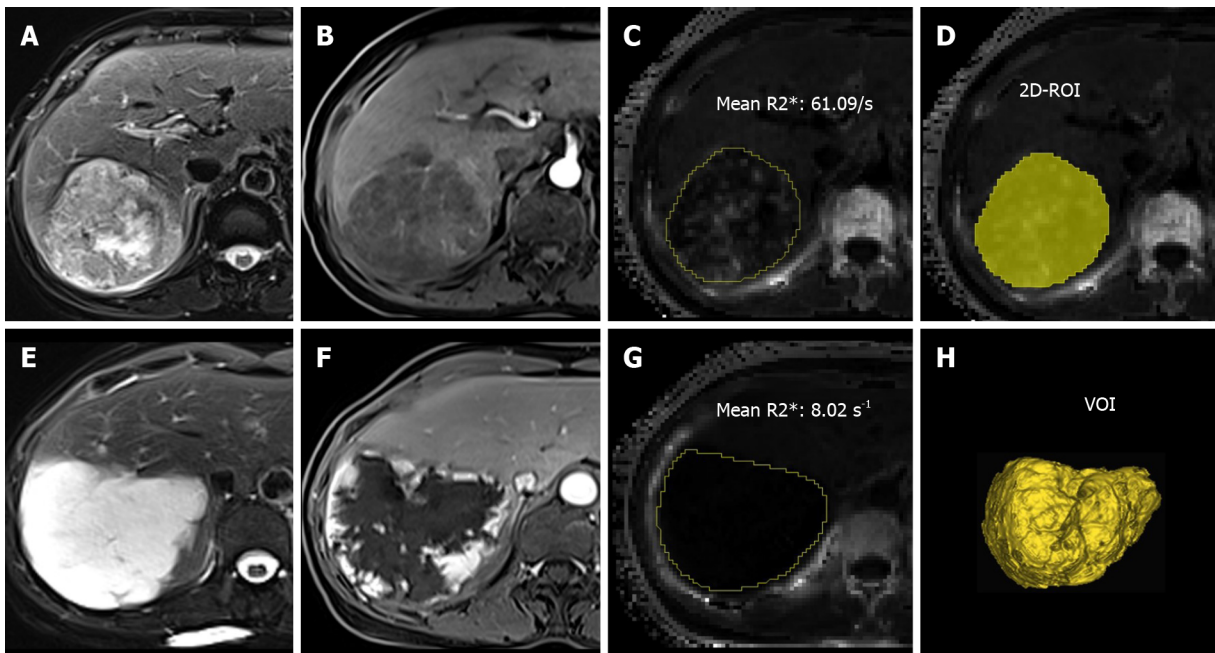


**Figure 1 Two-dimensional region of interest and volume of interest.** A-C: T2-weighted imaging (T2WI) (A), arterial phase contrast-enhanced T1-weighted imaging (T1WI) (B), and R2\* map showed liver metastasis (yellow line) (C) confirmed by histology in a 59-year-old woman with lung cancer; D: Two-dimensional region of interest was drawn on the section showing the maximal tumor dimension; E-G: T2WI (E), arterial phase contrast-enhanced T1WI (F), and R2\* map showed a liver hemangioma (yellow line) (G) in a 59-year-old woman; H: Volume of interest was placed covering the entire tumor volume on R2\* map. 2D-ROI: Two-dimensional region of interest; VOI: Volume of interest.

### Diagnosis of FLLs

All analyzed lesions were diagnosed by contrast-enhanced MRI, follow-up contrast-enhanced CT/MRI examination within at least 6 mo, fluorine 18 ( $^{18}\text{F}$ ) fluorodeoxyglucose (FDG) PET-CT, or histopathological findings (hepatectomy or biopsy)<sup>[5,22-25]</sup>. Diagnostic reference standard was established based on histopathological confirmation in 29/32 hepatocellular carcinomas (HCCs), 6/9 intrahepatic cholangiocarcinomas (IHCCs), 7/37 metastases, 5/25 hemangiomas, and 2/3 focal nodular hyperplasias (FNHs). In the remaining 69 FLLs without histopathological results, diagnoses were established by well-accepted imaging findings in all acquired MRI sequences (*e.g.*, T1WI, T2WI, T2-SPAIR, DWI, and contrast-enhanced T1WI). Criteria were determined by consensus reading of two experienced radiologists (R1, Shi GZ; and R2, Gao M) by consideration of all acquired images. Further reference standards were required: (1) FFLs were diagnosed as primary malignant FFLs if they showed (a) characteristic imaging appearance during a 6-mo imaging follow-up combined with (b) clinical symptoms and serological results; (2) FFLs were diagnosed as liver metastasis in patients with primary malignancies (pathologically confirmed) when at least one of the following criteria was satisfied: (a) Newly developed lesion or an increase in size with typical imaging appearance during a 6-mo imaging follow-up; and (b) abnormal  $^{18}\text{F}$  FDG uptake at PET-CT examination; and (3) FFLs were diagnosed as benign lesions if (a) they were stable at 6-mo imaging follow-up with characteristic imaging appearance in subjects at low risk; and (b) no malignant tumor was found in patients with benign FLLs during imaging examination.

Three HCCs, three IHCCs, and 19 metastases were diagnosed according to 6-mo imaging follow-up. Eleven metastases were confirmed by PET-CT. In liver metastasis patients, the primary tumors were bladder cancer ( $n = 9$ ), lung cancer ( $n = 2$ ), colorectal cancer ( $n = 7$ ), cervical cancer ( $n = 4$ ), gastric cancer ( $n = 3$ ), gallbladder cancer ( $n = 1$ ), breast cancer ( $n = 1$ ), and HCC ( $n = 10$ ). For benign FLLs, 20 hemangiomas and one FNH were confirmed by 6-mo imaging follow-up. Two liver abscesses had typical imaging findings in all the MRI sequences and typical imaging findings in a 6-mo follow-up MRI examination after clinical treatment.

### Statistical analysis

Numerical data are expressed as the mean  $\pm$  SD. The Bland-Altman plot was performed to determine the interobserver agreement on R2\* measurements. Intraclass correlation coefficient (ICC) was used to determine the reliability between the two

radiologists in R2\* measurements using 2D-ROI and VOI methods (0-0.20 poor; 0.21-0.40 fair; 0.41-0.60 moderate; 0.61-0.80 good; and 0.81-1.0 excellent correlation). Mean R2\* values from the two readers were used for the final analysis. Nonparametric Mann-Whitney test was used to compare the difference in R2\* values between the malignant and benign groups. The receiver operating characteristic (ROC) analysis was used to evaluate the diagnostic performances of R2\*. The area under the ROC curve (AUC), optimal cut-off values, sensitivity, and specificity were determined as the maximum Youden index. Differences in the diagnostic performance of the two different ROI positioning methods were analyzed by comparing ROC curves according to the method developed by DeLong *et al*<sup>[26]</sup>.  $P < 0.05$  (two-tail) indicated a statistically significant difference.

## RESULTS

### Clinicopathological characteristics

A total of 108 FLLs were found in 73 patients, including 78 malignant FLLs (mean maximum diameter,  $48.2 \pm 37.7$  mm; range, 11-163 mm) and 30 benign FLLs (mean maximum diameter,  $32.3 \pm 22.5$  mm; range, 14-94 mm). Forty-nine patients had malignant FLLs (30 men and 19 women; mean age,  $56.3 \pm 10.3$  years; range, 40-81 years), and 24 patients (11 men and 13 women; mean age,  $52.1 \pm 12.9$  years; range, 31-73 years) had benign FLLs. The malignant FLLs included 32 HCCs, nine IHCCs, and 37 liver metastases. Benign FLLs included 25 hemangiomas, three FNHs, and two liver abscesses. The mean maximum diameter of liver metastases, HCCs, and IHCCs was  $29.1 \pm 24.1$  mm (range, 11-122 mm),  $66.3 \pm 43.0$  mm (range, 15-163 mm), and  $61.9 \pm 25.9$  mm (range, 32-111 mm), respectively. In benign FLLs, the mean maximum diameter of hemangiomas, FNHs, and liver abscesses was  $29.4 \pm 21.8$  mm (range, 14-94 mm),  $32.0 \pm 8.5$  mm (range, 23-40 mm), and  $69.5 \pm 12.0$  mm (range, 61-78 mm), respectively. Clinicopathological characteristics and laboratory evaluations of FLLs are shown in Tables 1 and 2.

### R2\* analysis

Figure 2 shows the Bland-Altman plot measurement of R2\* of FLLs for the two readers. For 2D-ROI analysis, the 95% limits of agreement of R2\* for the two readers were from -5.68 to 5.04/s, and the mean difference for the two readers was -0.32/s. For VOI analysis, the 95% limits of agreement of R2\* for the two readers were from -3.65 to 3.28/s, and the mean difference for the two readers was -0.18/s. The differences between the two readers using two different methods were relatively small. ICC for the 2D-ROI method was 0.994 and ICC for the VOI method was 0.998. The interobserver agreement was excellent.

The mean R2\* values measured by 2D-ROI and VOI methods were significantly higher in the malignant group than in the benign group (2D-ROI:  $37.99 \pm 17.71$  vs  $18.6 \pm 8.43$ /s,  $P < 0.001$ ; VOI:  $41.11 \pm 19.01$  vs  $20.61 \pm 9.01$ /s,  $P < 0.001$ ). For 2D-ROI measurement, the mean R2\* value of liver metastases was  $44.17 \pm 21.90$ /s, and the mean R2\* values of HCCs and IHCCs were  $33.45 \pm 10.15$  and  $28.72 \pm 10.21$ /s, respectively. The mean R2\* values of hemangiomas, FNHs, and abscesses were  $16.66 \pm 8.18$ ,  $26.21 \pm 5.61$ , and  $23.29 \pm 9.31$ /s, respectively. For VOI measurement, FLLs had a mean R2\* value of  $48.42 \pm 23.61$ /s for liver metastases,  $35.41 \pm 10.04$ /s for HCCs,  $31.34 \pm 9.65$ /s for IHCCs,  $19.36 \pm 8.93$ /s for hemangiomas,  $27.87 \pm 7.46$ /s for FNHs, and  $25.29 \pm 10.46$ /s for abscesses. Malignant FLLs had higher R2\* values than benign FLLs regardless of ROI placement methods (Table 3).

### ROC analysis

The AUC of 2D-ROI was 0.884 (95% CI, 0.819 to 0.950) at a cut-off of 25.2/s, with a sensitivity of 84.6% and specificity of 80.0% for differentiating benign from malignant FLLs. The VOI method yielded an AUC of 0.875 (95% CI: 0.806 to 0.945) at a cut-off of 26.7/s in distinguishing benign from malignant FLLs, with a sensitivity of 85.9% and specificity of 76.7%. There was no significant difference between the AUCs for 2D-ROI and VOI positioning methods for discriminating benign from malignant FLLs ( $Z = 1.069$ ,  $P = 0.285$ ) (Figure 3).

Table 1 Baseline characteristics of malignant and benign focal liver lesions of 73 patients

Characteristic	Malignant	Benign	Total
Per-patient basis			
No. of patients (%)	49 (67.1)	24 (32.9)	73
Age (yr)			
mean $\pm$ SD	56.3 $\pm$ 10.3	52.1 $\pm$ 12.9	55.0 $\pm$ 11.2
Range	40-81	31-73	31-81
Sex, n (%)			
Male	30 (61.2)	11 (45.8)	41
Female	19 (38.8)	13 (54.2)	32
Per-lesion basis			
No. of lesions	78 (72.3)	30 (27.8)	108
Maximum diameter (mm)			
mean $\pm$ SD	48.2 $\pm$ 37.7	32.3 $\pm$ 22.5	43.8 $\pm$ 34.8
Range	11-163	14-94	11-163
Methods of diagnosis (%)			
Pathology	42 (38.9)	7 (6.5)	49 (45.4)
Imaging follow-up	25 (23.1)	23 (21.3)	48 (44.4)
PET-CT	11 (10.2)	-	11 (10.2)

FLL: Focal liver lesion; PET-CT: Positron emission tomography-computed tomography.

## DISCUSSION

Our study showed that the mean R2\* value of malignant FLLs was significantly higher than that of the benign FLLs. R2\* derived from multi-echo Dixon imaging is a potential biomarker to differentiate malignant from benign FLLs.

The combined use of MRI, CT, and ultrasound has a high diagnostic performance for the identification of FLLs, but requires the administration of gadolinium or iodine contrast agents<sup>[7]</sup>. Gadolinium contrast is contraindicated in patients with severe renal impairment, because it may induce nephrogenic systemic fibrosis, and may even be a greater risk in patients with liver dysfunction<sup>[27,28]</sup>. Iodinated contrast administration for CT may aggravate renal failure<sup>[8]</sup>. Currently, no alternative imaging methods have been widely advocated for these patients. Hypoxia is an important factor in cancer progression, affecting the autonomous functions of tumor cells and nonautonomous processes such as angiogenesis, lymphangiogenesis, and inflammation<sup>[29]</sup>. Hypoxia causes an increase in the concentration of deoxygenated hemoglobin in the tumor. Deoxyhemoglobin can be used as an endogenous hypoxia tracer that may produce local magnetic field inhomogeneities to reduce T2\* relaxation time<sup>[30]</sup>. Furthermore, higher local deoxyhemoglobin may result in a decrease in proton T2\* relaxation time and a corresponding increase in R2\*, which indicates a link between R2\* and the oxygen concentration of local tissues<sup>[15]</sup>. Recently, susceptibility-weighted imaging, which was originally called blood-oxygen-level-dependent (BOLD) venographic imaging, has demonstrated advantages in the detection of hemorrhagic events due to its sensitivity to paramagnetic substances<sup>[31]</sup>. Also, BOLD MRI has shown ability in assessing tumor oxygenation and indirectly hypoxia, by detecting signal changes secondary to changes in blood flow and oxygenation<sup>[32]</sup>. These two sequences were commonly used in the central nervous system<sup>[33,34]</sup>. Currently, T2\* has been used in assessing tissue oxygenation status *in vivo* based on the paramagnetic properties of deoxyhemoglobin<sup>[35]</sup>. Besides, this technique has been shown to be feasible and accurate in the detection of HCC<sup>[27,32]</sup>.

Previously, R2\* values have been used to distinguish cancerous from normal prostatic regions, with higher mean R2\* values being related to a higher tumor Gleason score<sup>[36]</sup>. In addition, higher R2\* values were found in high-grade bladder cancer<sup>[15]</sup> and clear cell renal cell carcinoma<sup>[37]</sup> than those of low-grade malignancies. In

Table 2 Clinicopathological characteristics of 108 focal liver lesions

Characteristic	Malignant			Benign		
	HCC	IHCC	Hemangioma	FNH	Abscess	
No. of lesions (%)	32 (29.6)	9 (8.3)	37 (34.3)	25 (23.1)	3 (2.8)	2 (1.9)
Maximum diameter (mm)						
mean ± SD	66.3 ± 43.0	61.9 ± 5.9	29.1 ± 24.1	29.4 ± 21.8	32.0 ± 8.5	69.5 ± 12.0
Range	15-163	32-111	11-122	14-94	23-40	61-78
Methods of diagnosis (%)						
Pathology	29 (26.9)	6 (5.6)	7 (6.5)	5 (4.6)	2 (1.9)	0 (0)
Imaging follow-up	3 (2.8)	3 (2.8)	19 (17.6)	20 (18.5)	1 (0.9)	2 (1.9)
PET-CT	-	-	11 (10.2)	-	-	-
Viral infection						
HBV	30	6	34	9	1	2
Non-HBV	2	3	3	9	1	0
NA	0	0	0	7	1	0
Cirrhosis on pathology (%)						
Yes	25	-	-	-	-	-
No	1	-	-	-	-	-
NA	6	-	-	-	-	-
AFP (ng/mL)						
≤ 25	12	9	29	-	-	-
> 25	20	0	7	-	-	-
NA	0	0	1	-	-	-
CA 19-9 (U/mL)						
≤ 34	21	4	15	-	-	-
> 34	9	5	20	-	-	-
NA	2	0	2	-	-	-
CEA (ng/mL)						
≤ 5	27	7	15	-	-	-
> 5	5	2	22	-	-	-
NA	0	0	0	-	-	-

AFP: -fetoprotein; CA 19-9: Carbohydrate antigen 19-9; CEA: Carcinoma embryonic antigen; FFL: Focal liver lesion; FNH: Focal nodular hyperplasia; HBV: Hepatitis B virus; HCC: Hepatocellular carcinoma; IHCC: Intrahepatic cholangiocarcinoma; NA: Not available; PET-CT: Positron emission tomography-computed tomography. Data are shown as the mean SD.

our study, the mean R2\* value of malignant FLLs was significantly higher than that of the benign FLLs. This may be attributed to the rapid growth of liver malignancies, resulting in a relatively hypoxic state and an increase in deoxyhemoglobin<sup>[15]</sup>. Consequently, the corresponding increase in R2\* value may correlate with the degree of malignancy of FFL. R2\* may be used as a quantitative imaging biomarker to provide additional information for tumor differential diagnosis.

In our study, mean R2\* values, whether derived from 2D-ROI or VOI segmentation positioning methods, were highly reproducible. Moreover, the AUC of R2\* measured by 2D-ROI was 0.884 with a sensitivity of 84.6% and specificity of 80.0%, while AUC of R2\* measured by VOI yielded an AUC of 0.875 with a sensitivity of 85.9% and specificity of 76.7%, in distinguishing benign from malignant FFLs, respectively. Campo *et al*<sup>[38]</sup> demonstrated that a large ROI that refers to as large an area of the liver as possible can improve the reproducibility and repeatability of R2\* measurements in

Table 3 Mean R2\* values for different focal liver lesions

FLL	2D-ROI method	VOI method
Malignant		
Liver metastasis	44.17 ± 21.90	48.42 ± 23.61
HCC	33.45 ± 10.15	35.41 ± 10.04
IHCC	28.72 ± 10.21	31.34 ± 9.65
Benign		
Hemangioma	16.66 ± 8.18	19.36 ± 8.93
FNH	26.21 ± 5.61	27.87 ± 7.46
Abscess	23.29 ± 9.31	25.29 ± 10.46

Numerical data are expressed as the mean ± SD. 2D-ROI: Two-dimensional region of interest; FFL: Focal liver lesion; FNH: Focal nodular hyperplasia; HCC: Hepatocellular carcinoma; IHCC: Intrahepatic cholangiocarcinoma; VOI: Volume of interest.

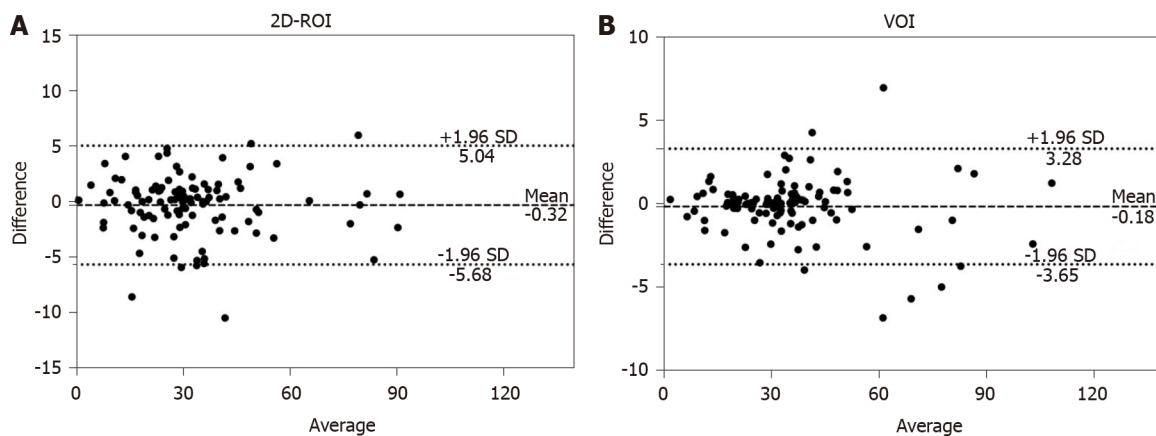


**Figure 2** Bland–Altman plots showing interobserver variability in two-dimensional region of interest and volume of interest measurements. A: Two-dimensional region of interest (ROI); B: Volume of interest. The differences between the two readers using the two different ROI positioning methods were small. 2D-ROI: Two-dimensional region of interest; VOI: Volume of interest.

patients with low and high liver iron content. McCarville *et al*<sup>[39]</sup> reported excellent interobserver agreements in liver R2\* for both small ( $\geq 1$  cm diameter) and whole liver ROI methods for iron overloaded patients who underwent biopsy. Sofue *et al*<sup>[40]</sup> found that R2\* measurements of whole liver volume and colocalized ROIs in three different hepatic segments were repeatable between examinations. However, these studies investigated ROI location of R2\* measurements in diffusive liver lesions rather than FLLs. To the best of our knowledge, our study was the first to investigate R2\* measurements in FLLs.

We found similar results in differentiating between benign and malignant FLLs by using 2D-ROI and VOI methods for R2\* measurement. ROC curve analysis demonstrated no significant difference between the AUCs for 2D-ROI and VOI positioning methods for discriminating benign from malignant FLLs. R2\* measured by VOI analysis showed an AUC of 0.875, while 2D-ROI analysis showed an AUC of 0.884 in differentiating between benign and malignant FLLs. These results indicate that the impact of the different ROI positioning methods could be ignored for the differential diagnosis of benign and malignant FLLs. Thust *et al*<sup>[41]</sup> obtained the same results in volumetric and 2D measurements of apparent diffusion coefficient in distinguishing glioma subtypes. Compared with VOI, 2D-ROI is easier to delineate and easily incorporated into clinical practice. The easy implementation of R2\* measurements using 2D-ROI will facilitate its clinical application.

There were several limitations to this study. First, this was a single-center study, and the number of patients in the cohort was relatively small. A larger patient cohort in a multicenter setting is needed to validate our findings. Second, R2\* is an indirect method for monitoring tumor PO<sub>2</sub><sup>[42]</sup>. In addition to the oxygenation state, R2\* can also

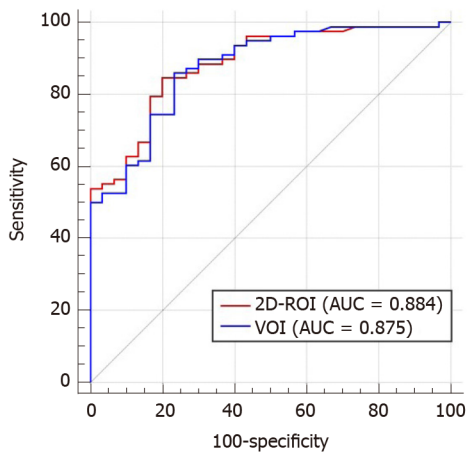


**Figure 3 Receiver operating characteristic curve analysis of the two positioning methods in differentiating between malignant group and benign group.** Two-dimensional region of interest and volume of interest methods yielded similar results. 2D-ROI: Two-dimensional region of interest; VOI: Volume of interest; AUC: Area under the curve.

be affected by other factors, such as hemoglobin levels, blood volume, and vasculature<sup>[15]</sup>. Nevertheless, various studies have found that T2WI is a highly sensitive technique for reliably assessing paramagnetic deoxyhemoglobin, methemoglobin, or hemosiderin in lesions and tissues in body imaging<sup>[30,35,37]</sup>. R2\* quantification can yield hypoxia information about malignancies in a noninvasive manner<sup>[19,42]</sup>. In addition, the sequence used in our study is easy to perform and requires only a single breath-hold of 16 s to image the entire liver, and no image postprocessing is required.

## CONCLUSION

In conclusion, R2\* values derived from multi-echo Dixon imaging can aid in discrimination between benign and malignant FLLs. 2D-ROI and VOI methods do not affect the diagnostic performance of R2\*. R2\* measured by 2D-ROI can be adopted to improve diagnostic accuracy of FFLs, particularly in patients with a contraindication to contrast agents.

## ARTICLE HIGHLIGHTS

### Research background

It is essential to distinguish between benign and malignant focal liver lesions (FLLs), as this differentiation determines the individual's prognosis and subsequent treatment strategy. Since the use of iodine and gadolinium-based contrast agents is contraindicated, imaging techniques without the need of contrast agents have been used to diagnose FFLs, including diffusion-weighted imaging, intravoxel incoherent motion, diffusion kurtosis imaging, and magnetic resonance elastography.

### Research motivation

Imaging techniques without the need of contrast agents have shown mixed success with limited clinical application. R2\* estimation is inversely related to partial tissue pressure of oxygen, and reflects the paramagnetism of the tumor tissue, which may be helpful to differentiate between benign and malignant FLLs.

### Research objectives

To investigate whether R2\* derived from multi-echo Dixon imaging can aid differentiating benign from malignant FLLs. The findings obtained can provide information for differential diagnosis of FLLs using R2\*.

### Research methods

This study retrospectively enrolled 73 patients with 108 benign or malignant FLLs. All patients underwent conventional abdominal magnetic resonance imaging and multi-

echo Dixon imaging. The mean R2\* values of lesions were measured using 2D region of interest (2D-ROI) and volume of interest (VOI) approaches. Mean R2\* values were compared between benign and malignant FLLs using the nonparametric Mann-Whitney test. Receiver operating characteristic curve analysis was used to determine the diagnostic performance of R2\* in differentiation between benign and malignant FLLs. The diagnostic performance of R2\* measured by 2D-ROI and VOI approaches was compared.

### Research results

The study included 30 benign and 78 malignant FLLs. Mean R2\* was significantly higher for malignant than benign FLLs as measured by 2D-ROI ( $P < 0.001$ ) and VOI ( $P < 0.001$ ). The area under the curve (AUC) of R2\* measured by 2D-ROI was 0.884 at a cut-off of 25.2/s, with a sensitivity of 84.6% and specificity of 80.0% for differentiating benign from malignant FLLs. R2\* measured by VOI yielded a AUC of 0.875 at a cut-off of 26.7/s in distinguishing benign from malignant FLLs, with a sensitivity of 85.9% and specificity of 76.7%. The AUCs of R2\* were not significantly different between the 2D-ROI and VOI methods. However, due to the relatively small sample size, a large population from multiple centers is needed for further validation of our findings.

### Research conclusions

R2\* derived from multi-echo Dixon imaging can aid in differentiation between benign and malignant FLLs. 2D-ROI and VOI methods do not affect the diagnostic performance of R2\*.

### Research perspectives

This study describes that R2\* value derived from multi-echo Dixon imaging can aid in differentiation between benign and malignant FLLs. The multi-echo Dixon sequence is easy to perform and requires only a single breath-hold of 16 s to image the entire liver, which holds a good potential for clinical application.

## REFERENCES

- 1 **Bray F**, Ferlay J, Soerjomataram I, Siegel RL, Torre LA, Jemal A. Global cancer statistics 2018: GLOBOCAN estimates of incidence and mortality worldwide for 36 cancers in 185 countries. *CA Cancer J Clin* 2018; **68**: 394-424 [PMID: 30207593 DOI: 10.3322/caac.21492]
- 2 **Landreau P**, Drouillard A, Launoy G, Ortega-Deballon P, Jooste V, Lepage C, Faivre J, Facy O, Bouvier AM. Incidence and survival in late liver metastases of colorectal cancer. *J Gastroenterol Hepatol* 2015; **30**: 82-85 [PMID: 25088563 DOI: 10.1111/jgh.12685]
- 3 **Dong Y**, Zhang XL, Mao F, Huang BJ, Si Q, Wang WP. Contrast-enhanced ultrasound features of histologically proven small ( $\leq 20$  mm) liver metastases. *Scand J Gastroenterol* 2017; **52**: 23-28 [PMID: 27577113 DOI: 10.1080/00365521.2016.1224380]
- 4 **Choi SH**, Lee SS, Park SH, Kim KM, Yu E, Park Y, Shin YM, Lee MG. LI-RADS Classification and Prognosis of Primary Liver Cancers at Gadoteric Acid-enhanced MRI. *Radiology* 2019; **290**: 388-397 [PMID: 30422088 DOI: 10.1148/radiol.2018181290]
- 5 **Tang A**, Bashir MR, Corwin MT, Cruite I, Dietrich CF, Do RKG, Ehman EC, Fowler KJ, Hussain HK, Jha RC, Karam AR, Mamidipalli A, Marks RM, Mitchell DG, Morgan TA, Ohliger MA, Shah A, Vu KN, Sirlin CB; LI-RADS Evidence Working Group. Evidence Supporting LI-RADS Major Features for CT- and MR Imaging-based Diagnosis of Hepatocellular Carcinoma: A Systematic Review. *Radiology* 2018; **286**: 29-48 [PMID: 29166245 DOI: 10.1148/radiol.2017170554]
- 6 **Semelka RC**, Martin DR, Balci C, Lance T. Focal liver lesions: comparison of dual-phase CT and multisequence multiplanar MR imaging including dynamic gadolinium enhancement. *J Magn Reson Imaging* 2001; **13**: 397-401 [PMID: 11241813 DOI: 10.1002/jmri.1057]
- 7 **Westwood M**, Joore M, Grutters J, Redekop K, Armstrong N, Lee K, Gloy V, Raatz H, Misso K, Severens J, Kleijnen J. Contrast-enhanced ultrasound using SonoVue® (sulphur hexafluoride microbubbles) compared with contrast-enhanced computed tomography and contrast-enhanced magnetic resonance imaging for the characterisation of focal liver lesions and detection of liver metastases: a systematic review and cost-effectiveness analysis. *Health Technol Assess* 2013; **17**: 1-243 [PMID: 23611316 DOI: 10.3310/hta17160]
- 8 **Thomsen HS**. Imaging patients with chronic kidney disease: CIN or NSF? *Radiol Med* 2007; **112**: 621-625 [PMID: 17653629 DOI: 10.1007/s11547-007-0168-y]
- 9 **Marckmann P**, Skov L, Rossen K, Dupont A, Damholt MB, Heaf JG, Thomsen HS. Nephrogenic systemic fibrosis: suspected causative role of gadodiamide used for contrast-enhanced magnetic resonance imaging. *J Am Soc Nephrol* 2006; **17**: 2359-2362 [PMID: 16885403 DOI: 10.1681/ASN.2006060601]
- 10 **Onur MR**, Çiçekçi M, Kayalı A, Poyraz AK, Kocakoç E. The role of ADC measurement in

- differential diagnosis of focal hepatic lesions. *Eur J Radiol* 2012; **81**: e171-e176 [PMID: 21353418 DOI: 10.1016/j.ejrad.2011.01.116]
- 11 **Choi IY**, Lee SS, Sung YS, Cheong H, Lee H, Byun JH, Kim SY, Lee SJ, Shin YM, Lee MG. Intravoxel incoherent motion diffusion-weighted imaging for characterizing focal hepatic lesions: Correlation with lesion enhancement. *J Magn Reson Imaging* 2017; **45**: 1589-1598 [PMID: 27664970 DOI: 10.1002/jmri.25492]
  - 12 **Rosenkrantz AB**, Sigmund EE, Winnick A, Niver BE, Spieler B, Morgan GR, Hajdu CH. Assessment of hepatocellular carcinoma using apparent diffusion coefficient and diffusion kurtosis indices: preliminary experience in fresh liver explants. *Magn Reson Imaging* 2012; **30**: 1534-1540 [PMID: 22819175 DOI: 10.1016/j.mri.2012.04.020]
  - 13 **Hennedige TP**, Hallinan JT, Leung FP, Teo LL, Iyer S, Wang G, Chang S, Madhavan KK, Wee A, Venkatesh SK. Comparison of magnetic resonance elastography and diffusion-weighted imaging for differentiating benign and malignant liver lesions. *Eur Radiol* 2016; **26**: 398-406 [PMID: 26032879 DOI: 10.1007/s00330-015-3835-8]
  - 14 **Tatum JL**, Kelloff GJ, Gillies RJ, Arbeit JM, Brown JM, Chao KS, Chapman JD, Eckelman WC, Fyles AW, Giaccia AJ, Hill RP, Koch CJ, Krishna MC, Krohn KA, Lewis JS, Mason RP, Melillo G, Padhani AR, Powis G, Rajendran JG, Reba R, Robinson SP, Semenza GL, Swartz HM, Vaupel P, Yang D, Croft B, Hoffman J, Liu G, Stone H, Sullivan D. Hypoxia: importance in tumor biology, noninvasive measurement by imaging, and value of its measurement in the management of cancer therapy. *Int J Radiat Biol* 2006; **82**: 699-757 [PMID: 17118889 DOI: 10.1080/09553000601002324]
  - 15 **Wang Y**, Shen Y, Hu X, Li Z, Feng C, Hu D, Kamel IR. Application of R2\* and Apparent Diffusion Coefficient in Estimating Tumor Grade and T Category of Bladder Cancer. *AJR Am J Roentgenol* 2020; **214**: 383-389 [PMID: 31670586 DOI: 10.2214/AJR.19.21668]
  - 16 **Santarelli MF**, Meloni A, De Marchi D, Pistoia L, Quarta A, Spasiano A, Landini L, Pepe A, Positano V. Estimation of pancreatic R2\* for iron overload assessment in the presence of fat: a comparison of different approaches. *MAGMA* 2018; **31**: 757-769 [PMID: 30043125 DOI: 10.1007/s10334-018-0695-7]
  - 17 **Krishna MC**, Subramanian S, Kuppusamy P, Mitchell JB. Magnetic resonance imaging for *in vivo* assessment of tissue oxygen concentration. *Semin Radiat Oncol* 2001; **11**: 58-69 [PMID: 11146043 DOI: 10.1053/srao.2001.18104]
  - 18 **Schmeel FC**, Luetkens JA, Feißt A, Enkirch SJ, Endler CH, Wagenhäuser PJ, Schmeel LC, Träber F, Schild HH, Kukuk GM. Quantitative evaluation of T2\* relaxation times for the differentiation of acute benign and malignant vertebral body fractures. *Eur J Radiol* 2018; **108**: 59-65 [PMID: 30396672 DOI: 10.1016/j.ejrad.2018.09.021]
  - 19 **Liu M**, Guo X, Wang S, Jin M, Wang Y, Li J, Liu J. BOLD-MRI of breast invasive ductal carcinoma: correlation of R2\* value and the expression of HIF-1 $\alpha$ . *Eur Radiol* 2013; **23**: 3221-3227 [PMID: 23835924 DOI: 10.1007/s00330-013-2937-4]
  - 20 **Korteweg MA**, Zwanenburg JJ, Hoogduin JM, van den Bosch MA, van Diest PJ, van Hillegersberg R, Eijkemans MJ, Mali WP, Luijten PR, Veldhuis WB. Dissected sentinel lymph nodes of breast cancer patients: characterization with high-spatial-resolution 7-T MR imaging. *Radiology* 2011; **261**: 127-135 [PMID: 21673230 DOI: 10.1148/radiol.11103535]
  - 21 **Zhao YZ**, Gan YG, Zhou JL, Liu JQ, Cao WG, Cheng SM, Bai DM, Wang MZ, Gao FQ, Zhou SM. Accuracy of multi-echo Dixon sequence in quantification of hepatic steatosis in Chinese children and adolescents. *World J Gastroenterol* 2019; **25**: 1513-1523 [PMID: 30948914 DOI: 10.3748/wjg.v25.i12.1513]
  - 22 **Renzulli M**, Clemente A, Ierardi AM, Pettinari I, Tovoli F, Brocchi S, Peta G, Cappabianca S, Carrafiello G, Golfieri R. Imaging of Colorectal Liver Metastases: New Developments and Pending Issues. *Cancers (Basel)* 2020; **12** [PMID: 31936319 DOI: 10.3390/cancers12010151]
  - 23 **Ta CN**, Kono Y, Eghtedari M, Oh YT, Robbin ML, Barr RG, Kummel AC, Mattrey RF. Focal Liver Lesions: Computer-aided Diagnosis by Using Contrast-enhanced US Cine Recordings. *Radiology* 2018; **286**: 1062-1071 [PMID: 29072980 DOI: 10.1148/radiol.2017170365]
  - 24 **Agnello F**, Ronot M, Valla DC, Sinkus R, Van Beers BE, Vilgrain V. High-b-value diffusion-weighted MR imaging of benign hepatocellular lesions: quantitative and qualitative analysis. *Radiology* 2012; **262**: 511-519 [PMID: 22143926 DOI: 10.1148/radiol.11110922]
  - 25 **Mortele KJ**, Ros PR. Benign liver neoplasms. *Clin Liver Dis* 2002; **6**: 119-145 [PMID: 11933585 DOI: 10.1016/s1089-3261(03)00069-2]
  - 26 **DeLong ER**, DeLong DM, Clarke-Pearson DL. Comparing the areas under two or more correlated receiver operating characteristic curves: a nonparametric approach. *Biometrics* 1988; **44**: 837-845 [PMID: 3203132]
  - 27 **Hardie AD**, Romano PB. The use of T2\*-weighted multi-echo GRE imaging as a novel method to diagnose hepatocellular carcinoma compared with gadolinium-enhanced MRI: a feasibility study. *Magn Reson Imaging* 2010; **28**: 281-285 [PMID: 20071122 DOI: 10.1016/j.mri.2009.12.010]
  - 28 **Shenoy C**. Gadolinium-induced nephrogenic systemic fibrosis in patients with kidney and liver disease. *Am J Med* 2008; **121**: e11; author reply e13 [PMID: 18187056 DOI: 10.1016/j.amjmed.2007.07.030]
  - 29 **Avni R**, Cohen B, Neeman M. Hypoxic stress and cancer: imaging the axis of evil in tumor metastasis. *NMR Biomed* 2011; **24**: 569-581 [PMID: 21793071 DOI: 10.1002/nbm.1632]
  - 30 **Chavhan GB**, Babyn PS, Thomas B, Shroff MM, Haacke EM. Principles, techniques, and applications of T2\*-based MR imaging and its special applications. *Radiographics* 2009; **29**: 1433-

- 1449 [PMID: 19755604 DOI: 10.1148/rg.295095034]
- 31 **Lou M**, Chen Z, Wan J, Hu H, Cai X, Shi Z, Sun J. Susceptibility-diffusion mismatch predicts thrombolytic outcomes: a retrospective cohort study. *AJNR Am J Neuroradiol* 2014; **35**: 2061-2067 [PMID: 25012670 DOI: 10.3174/ajnr.A4017]
  - 32 **Jhaveri KS**, Cleary SP, Fischer S, Haider MA, Pargoankar V, Khalidi K, Moshonov H, Gallinger S. Blood oxygen level-dependent liver MRI: can it predict microvascular invasion in HCC? *J Magn Reson Imaging* 2013; **37**: 692-699 [PMID: 23125092 DOI: 10.1002/jmri.23858]
  - 33 **Schwarz D**, Bendszus M, Breckwoldt MO. Clinical Value of Susceptibility Weighted Imaging of Brain Metastases. *Front Neurol* 2020; **11**: 55 [PMID: 32117017 DOI: 10.3389/fneur.2020.00055]
  - 34 **Chaudhry AA**, Naim S, Gul M, Chaudhry A, Chen M, Jandial R, Badie B. Utility of Preoperative Blood-Oxygen-Level-Dependent Functional MR Imaging in Patients with a Central Nervous System Neoplasm. *Radiol Clin North Am* 2019; **57**: 1189-1198 [PMID: 31582044 DOI: 10.1016/j.rcl.2019.07.006]
  - 35 **Min JH**, Kim CK, Park BK, Kim E, Kim B. Assessment of renal lesions with blood oxygenation level-dependent MRI at 3 T: preliminary experience. *AJR Am J Roentgenol* 2011; **197**: W489-W494 [PMID: 21862777 DOI: 10.2214/AJR.10.6319]
  - 36 **Wu LM**, Chen XX, Xuan HQ, Liu Q, Suo ST, Hu J, Xu JR. Feasibility and preliminary experience of quantitative T2\* mapping at 3.0 T for detection and assessment of aggressiveness of prostate cancer. *Acad Radiol* 2014; **21**: 1020-1026 [PMID: 25018074 DOI: 10.1016/j.acra.2014.04.007]
  - 37 **Zhang YD**, Wu CJ, Wang Q, Zhang J, Wang XN, Liu XS, Shi HB. Comparison of Utility of Histogram Apparent Diffusion Coefficient and R2\* for Differentiation of Low-Grade From High-Grade Clear Cell Renal Cell Carcinoma. *AJR Am J Roentgenol* 2015; **205**: W193-W201 [PMID: 26204307 DOI: 10.2214/AJR.14.13802]
  - 38 **Campo CA**, Hernando D, Schubert T, Bookwalter CA, Pay AJV, Reeder SB. Standardized Approach for ROI-Based Measurements of Proton Density Fat Fraction and R2\* in the Liver. *AJR Am J Roentgenol* 2017; **209**: 592-603 [PMID: 28705058 DOI: 10.2214/AJR.17.17812]
  - 39 **McCarville MB**, Hillenbrand CM, Loeffler RB, Smeltzer MP, Song R, Li CS, Hankins JS. Comparison of whole liver and small region-of-interest measurements of MRI liver R2\* in children with iron overload. *Pediatr Radiol* 2010; **40**: 1360-1367 [PMID: 20333511 DOI: 10.1007/s00247-010-1596-8]
  - 40 **Sofue K**, Mileto A, Dale BM, Zhong X, Bashir MR. Interexamination repeatability and spatial heterogeneity of liver iron and fat quantification using MRI-based multistep adaptive fitting algorithm. *J Magn Reson Imaging* 2015; **42**: 1281-1290 [PMID: 25920074 DOI: 10.1002/jmri.24922]
  - 41 **Thust SC**, Hassanein S, Bisdas S, Rees JH, Hyare H, Maynard JA, Brandner S, Tur C, Jäger HR, Yousry TA, Mancini L. Apparent diffusion coefficient for molecular subtyping of non-gadolinium-enhancing WHO grade II/III glioma: volumetric segmentation versus two-dimensional region of interest analysis. *Eur Radiol* 2018; **28**: 3779-3788 [PMID: 29572636 DOI: 10.1007/s00330-018-5351-0]
  - 42 **Chopra S**, Foltz WD, Milosevic MF, Toi A, Bristow RG, Ménard C, Haider MA. Comparing oxygen-sensitive MRI (BOLD R2\*) with oxygen electrode measurements: a pilot study in men with prostate cancer. *Int J Radiat Biol* 2009; **85**: 805-813 [PMID: 19728195 DOI: 10.1080/09553000903043059]



Published by **Baishideng Publishing Group Inc**  
7041 Koll Center Parkway, Suite 160, Pleasanton, CA 94566, USA  
**Telephone:** +1-925-3991568  
**E-mail:** [bpgoffice@wjgnet.com](mailto:bpgoffice@wjgnet.com)  
**Help Desk:** <https://www.f6publishing.com/helpdesk>  
<https://www.wjgnet.com>

